

# A Compact Disc-Shaped Printed Antenna Using Parasitic Element on Ground Plane for Super Wideband Applications

M. M. Islam<sup>1</sup>, M. R. I. Faruque<sup>2</sup>, and M. T. Islam<sup>3</sup>

<sup>1</sup>Department of Software Engineering  
Daffodil International University, Dhanmondi, Dhaka 1207, Bangladesh  
mmoislam@yahoo.com

<sup>2</sup>Space Science Centre (ANGKASA)  
Universiti Kebangsaan Malaysia, 43600 UKM, Bangi, Selangor, Malaysia  
rashedgen@yahoo.com

<sup>3</sup>Department of Electrical, Electronic and Systems Engineering  
Universiti Kebangsaan Malaysia, 43600 UKM, Bangi, Selangor, Malaysia  
titareq@gmail.com

**Abstract** — A microstrip line-fed monopole antenna is proposed and investigated using a structure of parasitic element for super-wideband applications. The parasitic element consists of 4 rectangular embedded slots on the ground plane. This parasitic element on the ground plane leads the UWB frequency band into the SWB frequency band. This proposed monopole antenna is fed by a microstrip line and is printed on low dielectric FR4 material of 1.6 mm thickness. All the simulations are performed using commercially available, finite element method (FEM) based Ansoft high-frequency structure simulator (HFSS) software and CST Microwave Studio. Measured results exhibit that the proposed disc-shaped antenna shows a wide bandwidth which covers from 2.90 GHz to more than 20 GHz, with a compact dimension of 25 mm × 33 mm for VSWR <2, observing an extended ultra-wideband frequency. A good combination is noticed between simulation and measurement. This proposed SWB antenna delivers impedance bandwidth covering the L, C, X, Ku bands and points out sharply surface current flow and nearly omnidirectional radiation patterns, which is appropriate for UWB or SWB applications.

**Index Terms** — Microstrip line, parasitic element, Super Wide Band (SWB), Ultra-Wide Band (UWB).

## I. INTRODUCTION

The Federal Communications Commission (FCC) introduced the announcement of 3.1-10.6 GHz frequency band for commercial application of UWB technology [1]. The UWB antenna is the dominant figure of wireless communication and UWB technology. The utilization and the research of UWB antennas have been rising

sharply with the demand of the integration and miniaturization and the improvement of high-speed integrated circuits. Owing to various merits such as high data rate, high salvation to multi path interference, large band width, small emission power, remote sensing applications and low cost for short range access. Major differences are observed between UWB and SWB antennas. In the information warfare, SWB antenna plays an important role as a key component of electronic counterwork equipment, while UWB antenna is extensively applied in communication and impulse radar systems. UWB covers the frequency range from 3.1 to 10.6 GHz with a ratio bandwidth of 3.4:1, while more than 8:1 or 10:1 is the ratio bandwidth of the SWB antenna.

In the recent years, several ultra-wideband antennas have been reported [2-10]. These antennas have various designs of monopole structures, such as triangular [2], square [3-4], rectangular [5] semi-circle [6], and circular disc [7] monopole antennas. Some of these UWB antennas are not appropriate to be integrated with associated UWB electronics and some do not have simple structure and are not suitable to be integrated. And the typical feeding techniques include simple microstrip lines [8], CPW feeds [9], and slotted structures [10]. For these antenna design structures, the operations of the antenna are usually limited within 3.1-10.6 GHz UWB frequency range. In order to attain super wide frequency band, different methods and techniques have already been proposed. Recently, there are various literatures on SWB microstrip antennas [11-22]. For instance, in [11], a compact super wideband antenna was proposed with switchable dual band-notched characteristics for 3 to 33 GHz band. However, this

antenna contained no validation experimentally. A compact semielliptical antenna was proposed, which was fed by a tapered coplanar waveguide [12]. The mentioned antenna is appropriate to cover from 0.46 GHz to 9.07 GHz frequency with a measured bandwidth ratio of 19.7: 1. In [13], a circular shaped asymmetrical dipole antenna was presented. This reported antenna attained an operating frequency band covering from 0.79 to 17.46 GHz with a dimension of 90 mm  $\times$  135 mm. A novel SWB antenna was proposed, which achieved a frequency band from 5 GHz to 150 GHz in [14]. Although huge bandwidth exists, it is not appropriate for lower frequency bands such as S band communication and WiMAX. A half circular antenna of antipodal slot was designed with a range of 0.8 GHz to 7 GHz super wide band frequencies [15]. An asymmetrical dipole antenna of super-wideband was stated in [16]. A planar super wide band antenna of disc shape was designed with C-like slots in [17]. This mentioned antenna obtained bandwidth covering within 3-32 GHz with an overall dimension of 30 mm  $\times$  29:1 mm. An extremely wideband monopole antenna was designed with triple-band notched characteristics in [18]. The reported antenna acquired a bandwidth covering from 0.72-25 GHz with a size of 150 mm  $\times$  150 mm. In [19], a monopole antenna was presented for SWB applications. However, it's three dimensional structure makes it difficult to be integrated into portable devices. The peak gain is high but the antenna structure is too large. In addition, the reported [17-19] antennas do not cover K-band which introduces a new arena to design antenna that covers S, C, X, Ku, K and Ka bands. A monopole antenna was proposed for SWB applications [20]. This antenna covers the UWB demands including gain and bandwidth. At lower frequencies (2-2.5 GHz), the input impedance is not matched properly and the dimension is too large, that is 35 $\times$ 77 mm<sup>2</sup>. A SWB antenna was proposed with printed patch and tapered feed region in ref. [21]. The input impedance being mismatched at 18-19 GHz frequencies creates variant group delay and the antenna structure is too large, 40 $\times$ 30 mm<sup>2</sup>. A printed SWB antenna was presented and studied [22]. The overall antenna dimension is too large. A printed wideband antenna was narrated for multi-band wireless systems [23]. This antenna acquired wide bandwidth covering from 1:08 to 27:4 GHz, with a dimension of 124 mm  $\times$  120 mm  $\times$  1:5 mm. A monopole antenna of compact disc was designed for future UWB applications where operating bandwidth 3:5-31:9 GHz with a dimension of 35 mm  $\times$  30 mm  $\times$  0:8 mm [27]. An ultra-wideband antenna was proposed using capacitively loaded loop (CLL) with band-notched characteristics where covering bandwidth from 3 to 11 GHz with a dimension of 34 mm  $\times$  27 mm  $\times$  0:8 mm [25]. A printed ultra-wideband antenna was presented using inverted L-slit with band-notched characteristics where executing

frequency band 2:82-13:95 GHz with a dimension of 30 mm  $\times$  36 mm  $\times$  0:4 mm [26].

In this paper, a disc-shaped printed microstrip antenna with the parasitic element on the ground plane that attains a compact SWB profile physically belonging to nearly omni-directional radiation characteristics, gain and reasonable current distribution is presented. The mentioned disc-shaped SWB antenna is made of circular radiating patch and the ground plane containing the parasitic element on the upper portion, generating a super wide bandwidth ranging from 2.90 to more than 20 GHz. The antenna formation is smooth with simple design and comfortable fabrication. The parasitic element structure is inserted on the upper portion of the ground plane to generate super frequency band for SWB applications. By virtue of significant selection of the parasitic element structure, it is observed that the reported antenna can obtain the operating SWB frequency band.

## II. ANTENNA DESIGN ARCHITECTURE AND OPTIMIZATION

The geometrical outline of the proposed disc-shaped SWB antenna is demonstrated in Fig. 1, which is printed on both sides of a low cost dielectric, 1.6 mm thick FR4 substrate material belonging to permittivity of 4.6 and loss tangent 0.02. Finite element method (FEM) based Ansoft high-frequency structure simulator (HFSS) software, which is commercially available, has been used for all the simulations in this research. The reported SWB antenna has been designed following the UWB antenna1 indicated Fig. 2. This antenna is made of a disc-shaped radiating patch with a radius of R. The partial ground plane with the parasitic element is printed on the lower part of the substrate, where on the upper portion of the substrate; the disc-shaped radiator is printed using a microstrip line feeding.

The width and length of the microstrip line are stable with a view to attaining the 50  $\Omega$  input impedance. The port of the microstrip feed line is attached to a Sub Miniature version A (SMA) connector. The gap between the parasitic element and the partial ground plane is denoted using  $g_1$ .  $W_{sub} \times L_{sub} \times H_{sub}$  is the thorough size of the proposed SWB antenna. The parasitic element is implanted on the upper position of the partial ground plane to create super frequency band. The parasitic element is made of four embedded rectangular slots to achieve the characteristics of super wideband. However, the position of the parasitic element plays an important role in order to determine the super frequency band of the proposed SWB antenna. In case of SWB antenna structure, the function of the resonator is to create and control super wide frequency band sharply. Because of exhibiting these properties, this parasitic element is a perfect resonator structure. In spite of implanting this

parasitic structure, the thorough antenna size is unchanged where, for the perfect resonator structure, excessive space is no longer required.

The optimized value of the antenna design parameters are identified in Table 1. The proposed SWB antenna is positioned in the x-y plane as well as the normal direction is leaded as parallel to the z-axis in Fig. 1 (c). Basically, the patch was circular and some modifications were performed on the ground plane. To enhance the impedance bandwidth, the following measures are used as shown in Fig. 2.

- a) Adding a rectangular slot of about  $30^\circ$  angles, length of  $l_1$ , and width of 0.87 mm on the upper part of the ground plane as a parasitic element.
- b) Embedding a slot with length of  $w_1$ , width of 1 mm horizontally.
- c) Attaching a slot of about  $330^\circ$  with length of  $l_2$ , width of 1 mm.
- d) Adding a slot of  $30^\circ$  with length of 10.1 mm, width of 1.1 mm

By choosing the optimized parameters reported in Table 1, the proposed SWB antenna can be tuned for operating in SWB applications.

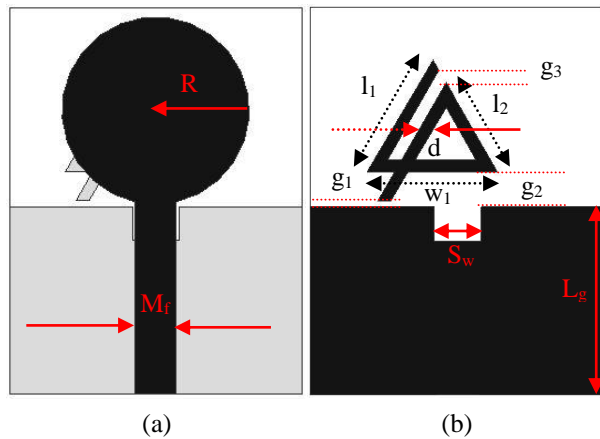


Fig. 1. The geometry of the proposed antenna: (a) top layer, (b) bottom layer, and (c) side view.

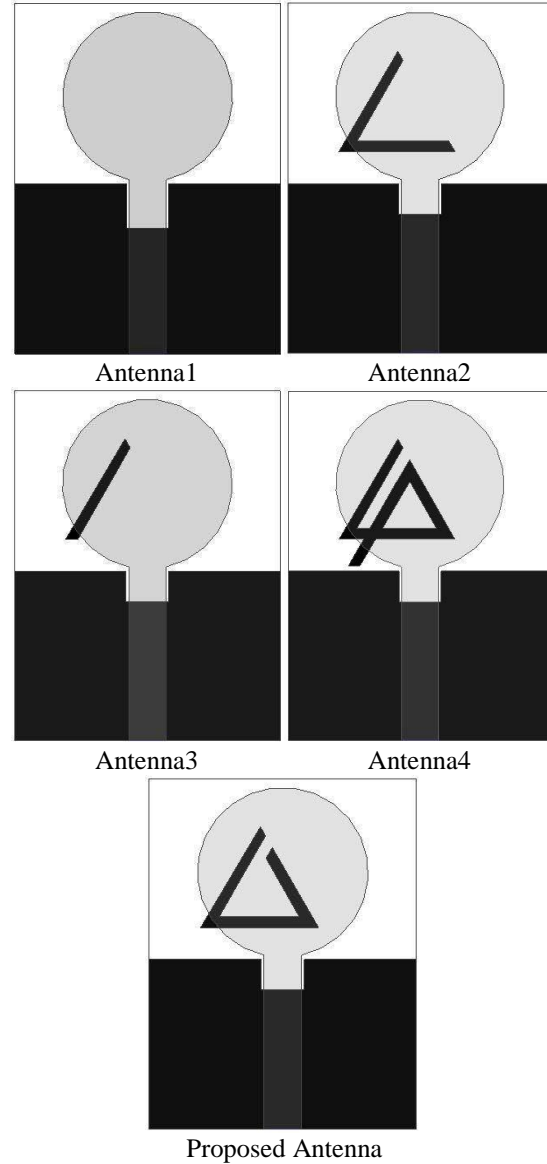


Fig. 2. The proposed design evolution with parasitic element.

Table 1: Optimized dimensions of the proposed SWB antenna

Para.	$L_{sub}$	$W_{sub}$	$H_{sub}$	$l_1$	$l_2$	$g_1$	$g_2$
mm	25	33	1.6	11	8.7	.5	3
Para.	$g_3$	$d$	$w_1$	$R$	$M_f$	$L_g$	$S_w$
mm	1.1	1.23	11.05	8	3.5	16	4

Figure 3 illustrates the input impedance of the various antenna structures with real values and the input impedance of the various antenna structures with imaginary values is indicated in Fig. 4. This SWB antenna is fed using a microstrip line of property impedance, which is referred before. It can be easily observed from the Fig. 3 that the impedance of the

proposed antenna with real values approaches to  $50 \Omega$  among all the antenna structures such as antenna 1, antenna 2, antenna 3 and antenna 4. On the other hand, it can be clearly seen from the Fig. 4 that the impedance of the proposed antenna with imaginary values approaches to zero among all the antenna structures such as antenna 1, antenna 2, antenna 3 and antenna 4. When the antenna impedance and the microstrip line property impedance approaches to both  $50 \Omega$ , the microstrip line impedance is matched with the load impedance. It can be found that this antenna impedance is well matched. The Fig. 5 shows the fabricated photograph of the proposed SWB antenna.

The simulated reflection coefficient property of various antenna structures is shown in Fig. 6. Antenna 1 covers frequency band from 2.9 GHz to 10.6 GHz and after that, covers 12.35 to 16.50 GHz. Antenna 2 covers 2.9-10.7 GHz frequency range and then again starts to operate from 12.1 GHz. Antenna 3 operates ranging from 2.9 to 4 GHz, 4.4 to 10.7 GHz and 12.2 to 18.9 GHz. Antenna 4 covers band from 3.08-10.7 GHz, 12.1-18.8 GHz and 19.4 GHz to more than 20 GHz. On the other hand, the proposed disc-shaped antenna covers from 2.9 GHz to more than 20 GHz, provides a reasonable wider impedance bandwidth in SWB applications in comparison to antenna 1, antenna 2, antenna 3 and antenna 4.

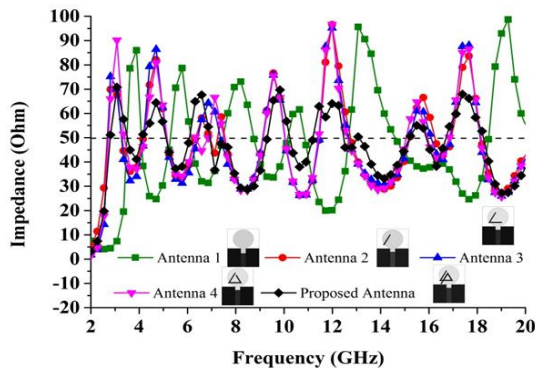


Fig. 3. Input impedance of the various antenna structures with real values.

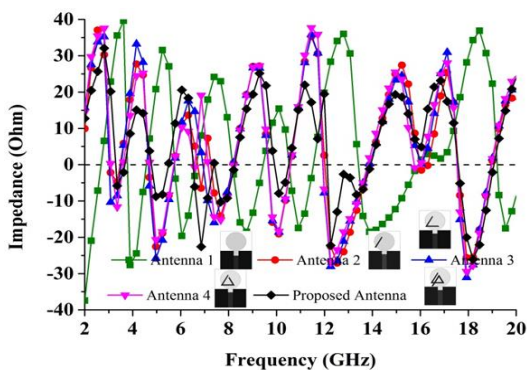


Fig. 4. Input impedance of the various antenna structures with imaginary values.

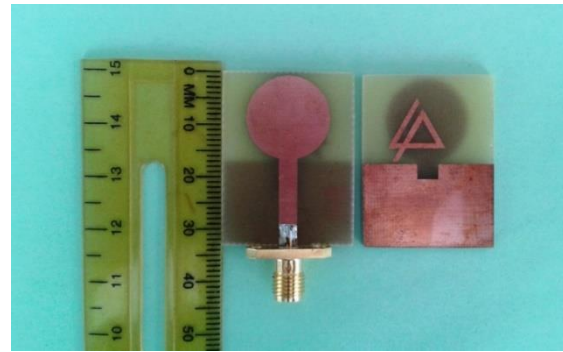


Fig. 5. The photograph of the top and bottom view of the proposed antenna.

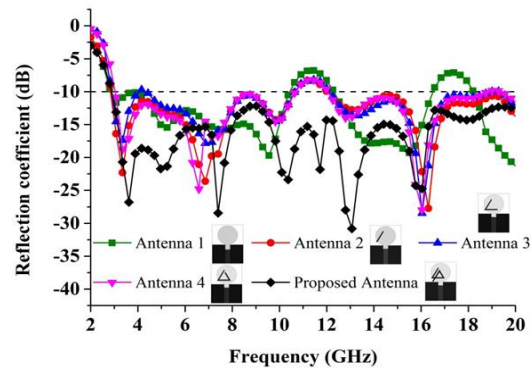


Fig. 6. simulated reflection coefficient properties of various antenna structures.

### III. RESULTS AND DISCUSSIONS

The performance characteristics of the proposed disc-shaped SWB antenna are explained, studied, and optimized using HFSS. The proposed disc-shaped antenna with the parasitic element on the ground plane is prototyped in the PCB LPKF (S63) prototyping machine to obtain a physical test model, which is illustrated in Fig. 7 (a). An anechoic chamber is acted as the most effective electromagnetic measurement system. The results of the proposed SWB antenna prototype are measured in a rectangular shaped anechoic chamber of dimensions  $5.5 \text{ m} \times 5 \text{ m} \times 3.5 \text{ m}$ . As a reference antenna, a double ridge guide horn antenna is adopted. During measurement this prototyped antenna is located face to face in respect to the reference antenna. Figure 7 (b) demonstrates the photograph of the anechoic chamber. A pyramidal-shaped electrically thick foam absorber is adopted on the wall, ceiling, and floor with less than  $-60 \text{ dB}$  reflectivity at normal incidence. A turntable of dimension 1.2 m diameter is applied in order to rotate the testing antenna with the specification, 3600 rotation angle, 1 RPM rotation speed was connected with a 10 meter cable among the controllers. An Agilent vector network analyzer (VNA E8362C) that covers up to 20 GHz is applied for the testing procedure.



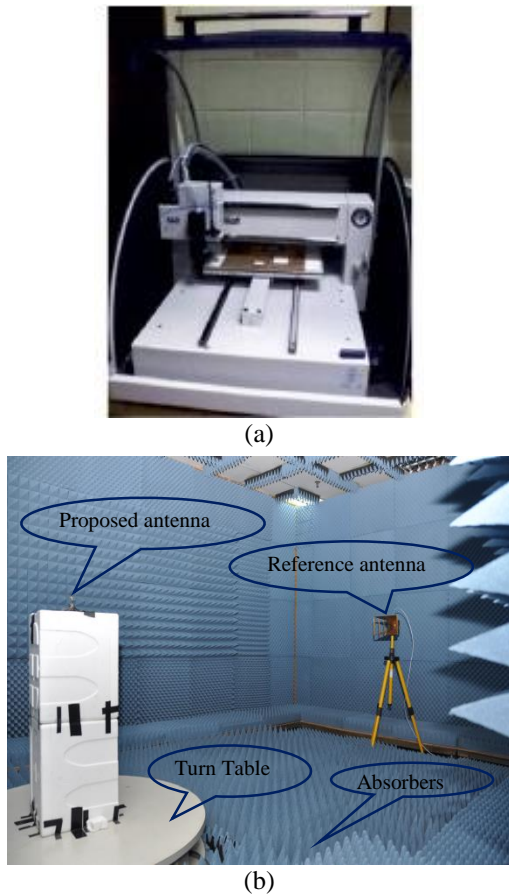


Fig. 7. (a) The LPKF machine and (b) the anechoic chamber for the proposed SWB antenna.

The simulated and measured reflection coefficient of the proposed SWB antenna is shown in Fig. 8. The measured results exhibit that the proposed disc-shaped antenna shows a broadband impedance matched properties which covers from 2.90 GHz to more than 20 GHz. The little discordance between the measurement and simulation results is owing to fabrication tolerance, extended ground effect and the effect of improper soldering of the SMA connector. However, the measured results are also almost coincidence with the expected results, so these results are adoptable.

The surface current distribution on the ground plane and the patch of the proposed SWB antenna at frequencies 3.5 GHz, 4.25 GHz, 9.9 GHz, 11.5 GHz, 13.3 GHz, and 17.75 GHz is illustrated respectively in Fig. 9 and Fig. 10. From Fig. 9, it is observed that the parasitic element on the upper portion of the ground plays an important role to create resonances and achieve super frequency bands. The parasitic element has a major effect at frequencies 3.5 GHz, 4.25 GHz, 11.5 GHz, and 13.3 GHz on the ground plane. This conducts to ensure that the performance of this SWB antenna is dependent on the parasitic element on the ground plane. Besides, the

amount of current flow exists also around the slot on the ground plane at frequencies 3.5 GHz, 4.25 GHz, 9.9 GHz and 11.5 GHz. The feeding line keeps the role to flow current sharply.

The surface current distribution on the patch at six frequencies is demonstrated in Fig. 10. It can be seen clearly from Fig. 10 that the microstrip feeding is a dominant figure and the disc-shaped patch also plays a role to flow current sharply. The surface current maintains a harmonic order flow both the patch and the ground plane. As a result, a super wide frequency band is generated.

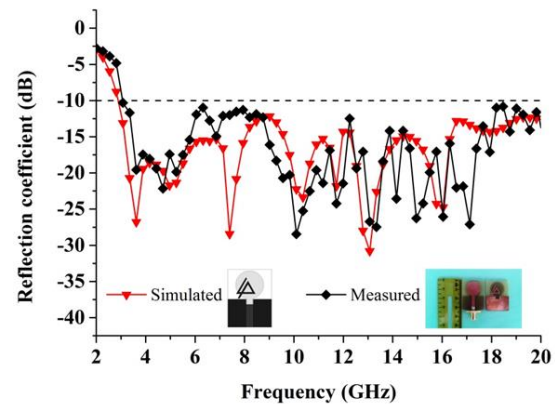
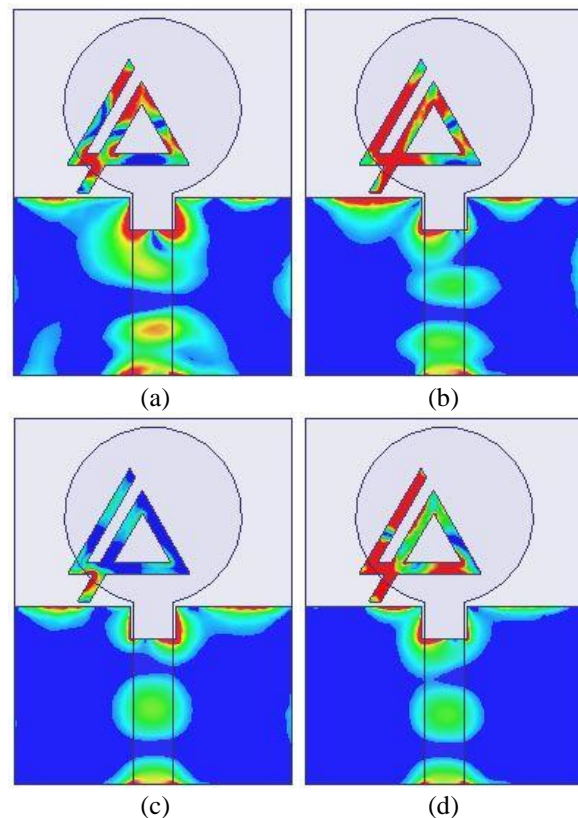


Fig. 8. Simulated and measured reflection coefficient of the proposed SWB antenna.



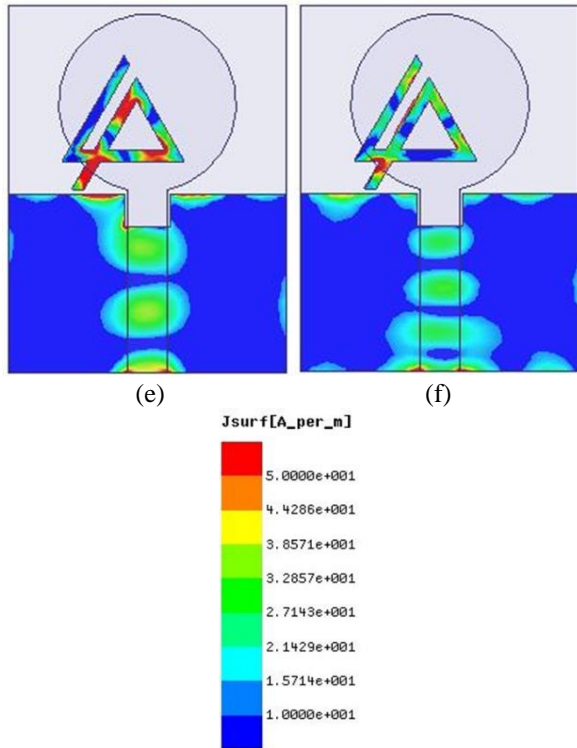


Fig. 9. Surface current distribution on the ground plane at frequencies: (a) 3.5 GHz, (b) 4.25 GHz, (c) 9.9 GHz, (d) 11.5 GHz, (e) 13.3 GHz, and (f) 17.75 GHz.

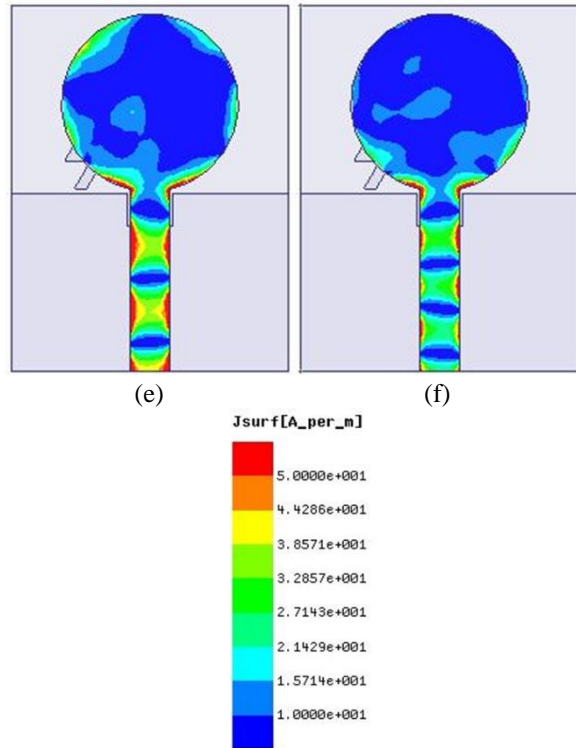
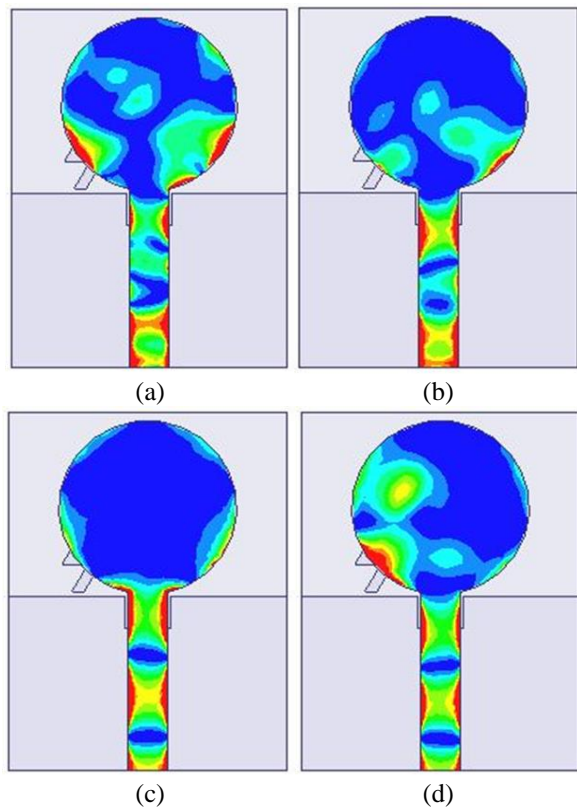


Fig. 10. Surface current distribution on the patch at frequencies: (a) 3.5 GHz, (b) 4.25 GHz, (c) 9.9 GHz, (d) 11.5 GHz, (e) 13.3 GHz, and (f) 17.75 GHz.



The measured normalized radiation pattern of the proposed disc-shaped SWB antenna is illustrated in Fig. 11 for (a) 3.5 GHz, (b) 4.25 GHz, (c) 9.9 GHz, (d) 11.5 GHz, (e) 13.3 GHz, and (f) 17.75 GHz on the both E-plane and H-plane, respectively. Two-dimensional (2D) radiation patterns are applied to indicate cross and co-polarization. To denote the co-polar and cross-polar,  $E_{\theta}$  and  $E_{\phi}$  are applied, respectively, where x-z plane is considered as H-plane and y-z plane is considered as E-plane. Cross-polarization is lower than co-polarization, which is the characteristic of standard radiation pattern. The cross-polarization has a higher effect on frequencies 11.5 GHz, 13.3 GHz at E-plane and frequencies 9.9 GHz, 17.75 GHz at H-plane. It is observed that the proposed SWB antenna exhibits better broadside radiation features, considerable front-to-back ratio with low cross polarization, which leads to symmetric and nearly omnidirectional radiation pattern along both the E-plane and the H-plane.

The proposed SWB antenna exhibits linear polarization, since the level of cross-polarization is lower than that of co-polarization in the radiation pattern. For this nearly omnidirectional radiation pattern characteristic, some reasonable merits are found. One merit is that the radiation pattern is more stable on the covering frequency. Resonances are not shifted all on a

sudden for various directions, so a stable amount of power exists in the direction of the broadside beam. The cross-polarization is comparatively higher in the radiation pattern, which may be happened due to the diffractions from the edges of the ground plane and the patch. These radiation patterns are appropriate for SWB applications.

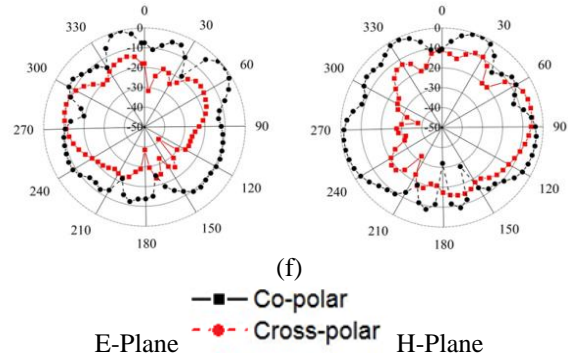
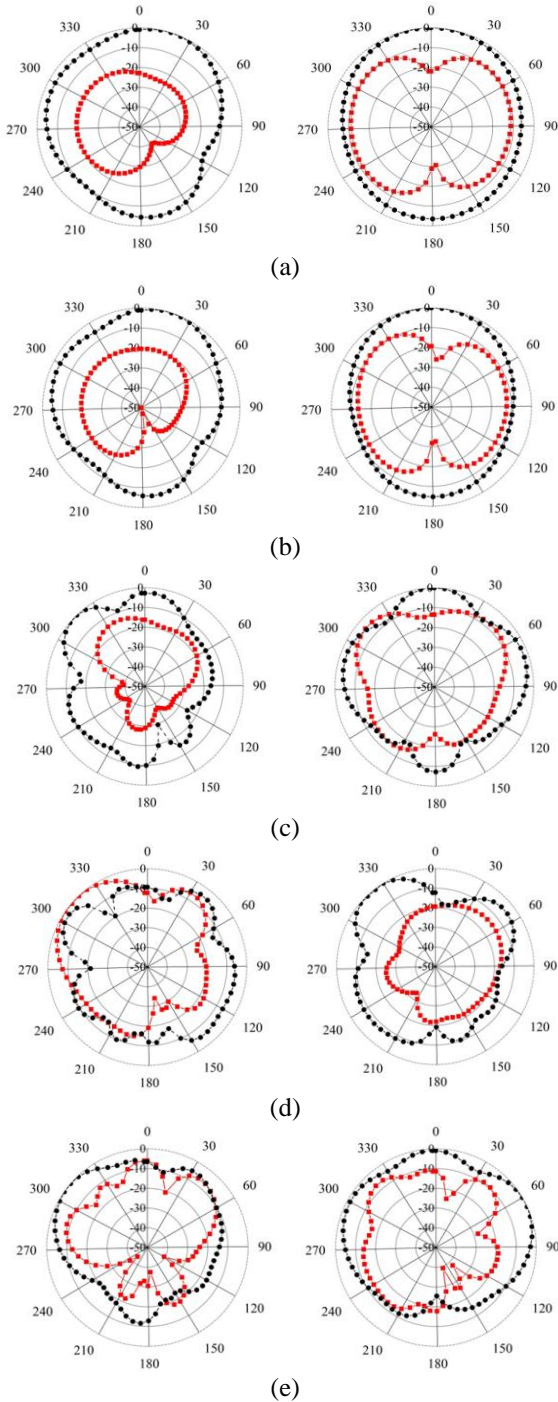


Fig. 11. Measured radiation pattern at frequencies: (a) 3.5 GHz, (b) 4.25 GHz, (c) 9.9 GHz, (d) 11.5 GHz, (e) 13.3 GHz, and (f) 17.75 GHz.

The measured gain of the proposed disc-shaped SWB antenna is exhibited in Fig. 12.

A standard three-antenna system is used for measuring gain with two identical horn antennas. It is known to the gains of the two identical horn antennas, and a gain with two identical horn antennas that follows well-known equations is applied in case of three antennas. The gain of the three antennas (under test) can be calculated following the below equations, because  $P_r$  is the radiated power, the gains of two horn antennas are known, and  $R$  is the distance between the two antennas.

Antenna 1 (horn) and Antenna 2 (horn):

$$G_1 + G_2 = 20 \log_{10} \left( \frac{4\pi R}{\lambda} \right) + 10 \log_{10} \left( \frac{P_{r2}}{P_{r1}} \right). \quad (1)$$

Antenna 1 (horn) and Antenna 3 (under test):

$$G_1 + G_3 = 20 \log_{10} \left( \frac{4\pi R}{\lambda} \right) + 10 \log_{10} \left( \frac{P_{r3}}{P_{r1}} \right). \quad (2)$$

Antenna 2 (horn) and Antenna 3 (under test):

$$G_2 + G_3 = 20 \log_{10} \left( \frac{4\pi R}{\lambda} \right) + 10 \log_{10} \left( \frac{P_{r3}}{P_{r2}} \right). \quad (3)$$

For directivity  $D$ , the following equation [41] is used in which  $U$  is the radiation intensity and  $P_{rad}$  is the total radiated power:

$$D = \frac{4\pi U}{P_{rad}}. \quad (4)$$

It can be observed clearly from the Fig. 12 that the average gain of the proposed SWB antenna is 3.78 dBi where the maximum peak gain is 6.22 dBi, which is accepted for SWB applications.

The phase value of the proposed disc-shaped SWB antenna is shown in Fig. 13. It can be observed from the graph that this phase values imply that all the frequency components of the signal belongs to the same pulse distortion due to the same propagation delay. As a result, the phase variation of this proposed SWB antenna is linear across the entire covering frequency bands 2.90 GHz to more than 20 GHz. Table 2 contains the comparison between the proposed and existing antennas.



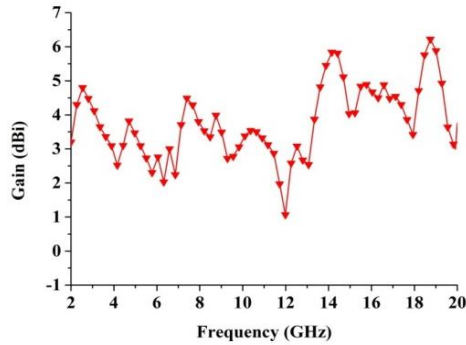


Fig. 12. Measured gain of the proposed disc-shaped SWB antenna.

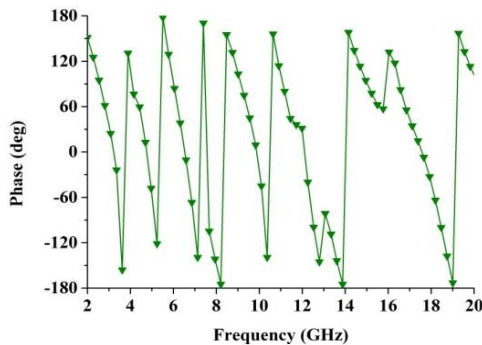


Fig. 13. The phase value of the proposed disc-shaped SWB antenna.

Table 2: Comparison between the proposed SWB and some existing antennas

Literature	Dimensions (mm <sup>2</sup> )	Pass Band (GHz)	Measured Gain (dBi)
[13]	90×135	0.7986-17.4663	-20 to 5
[20]	35×77	1.44-18.8	1 to 7
[21]	30×40	2.5-≥25	2 to 6
[23]	120×124	1.08-27.4	Not mentioned
[24]	25×35	3.5-31.9	-0.8 to 8
Proposed	25×33	2.90-≥20	3.20-6.22

#### IV. CONCLUSION

A disc-shaped monopole antenna is proposed and investigated with a design evolution analysis, implanting the parasitic element on the ground plane for SWB applications. This antenna comprises a disc-shaped radiating patch and a partial ground plane with the parasitic element and has an overall dimension of 25 mm × 33 mm. For planar structure, this proposed SWB antenna design is straight, comfort to fabricate, and very compatible to integrate into microwave circuitry. The parasitic element is used on the ground plane to achieve SWB frequency bands with nearly omni-directional radiation characteristics and smooth current distribution. It is realized experimentally that this antenna is matched

properly for SWB frequency ranging from 2.90 to more than GHz. The radiation patterns, low profile, stable gain and small dimension characteristics of the proposed antenna give the validation that, the reported antenna is a promising candidate of SWB applications.

#### REFERENCES

- [1] Federal Communications Commission Revision of Part 15 of the Commission's Rules Regarding Ultra-Wideband Transmission System from 3.1 to 10.6 GHz, in Federal Communications Commission: ET-Docket, pp. 98-153, 2002.
- [2] C.-C. Lin and H.-R. Chuang, "A 3-12 GHz UWB planar triangular monopole antenna with ridged ground-plane," *Progress In Electromagnetics Research*, vol. 83, pp. 191-198, 2008.
- [3] N. Ojaroudi, M. Ojaroudi, N. Ghadimi, and M. Mehranpour, "UWB square monopole antenna with omni-directional radiation patterns for use in circular cylindrical microwave imaging systems," *Applied Computational Electromagnetics Society (ACES) Journal*, vol. 28, no. 2, pp. 123-129, 2013.
- [4] N. Ojaroudi, M. Ojaroudi, and N. Ghadimi, "Square monopole antenna with band-notched characteristic for UWB communications," *Applied Computational Electromagnetics Society (ACES) Journal*, vol. 28, no. 8, pp. 712-718, 2013.
- [5] R. Azim, M. T. Islam, and N. Misran, "Design of a planar UWB antenna with new band enhancement technique," *Applied Computational Electromagnetics Society (ACES) Journal*, vol. 26, no. 10, 2011.
- [6] S. Lin, R.-N. Cai, G.-L. Huang, and J.-X. Wang, "A miniature UWB semi-circle monopole printed antenna," *Progress In Electromagnetics Research Letters*, vol. 23, pp. 157-163, 2011.
- [7] N. Ojaroudi, M. Ojaroudi, N. Ghadimi, "Disc shaped monopole antenna with dual band-notched function for UWB applications," *Applied Computational Electromagnetics Society (ACES) Journal*, vol. 28, no. 6, pp. 528-534, 2013.
- [8] M. M. Islam, M. T. Islam, M. Samsuzzaman, and M. R. I. Faruque, "Compact metamaterial antenna for UWB applications," *Electronics Letters*, vol. 51, pp. 1222-1224, 2015.
- [9] C. M. Li and L. H. Ye, "Improved dual band notched UWB slot antenna with controllable notched bandwidths," *Progress In Electromagnetics Research*, vol. 115, pp. 477-493, 2011.
- [10] M. T. Partovi, N. Ojaroudi, and M. Ojaroudi, "Small slot antenna with enhanced bandwidth and band-notched performance for UWB applications," *Applied Computational Electromagnetics Society (ACES) Journal*, vol. 27, no. 9, pp. 772-778, 2012.
- [11] M. Almkawi, M. Westrick, and V. Devabhaktuni, "Compact super wideband monopole antenna with



- switchable dual band-notched characteristics,” *Proceedings of the Asia-Pacific Microwave Conference*, Taiwan, pp. 723-725, 2012.
- [12] X. R. Yan, S. S. Zhong, and X. X. Yang, “Compact printed monopole antenna with super-wideband,” *Proceedings of the International Symposium on Microwave, Antenna, Propagation and EMC Technologies for Wireless Communications*, China, pp. 605-607, 2007.
- [13] S. Barbarino and F. Consoli, “UWB circular slot antenna provided with an inverted-L notch filter for the 5 GHz WLAN band,” *Progress In Electromagnetics Research*, vol. 104, pp. 1-13, 2010.
- [14] D. Tran, A. Szilagyi, I. E. Lager, P. Aubry, L. P. Ligthart, and A. Yarovoy, “A super wideband antenna,” *Proceedings of the 5<sup>th</sup> European Conference on Antennas and Propagation*, Italy, pp. 2656-2660, 2011.
- [15] W. Lu and H. Zhu, “Super-wideband antipodal slot antenna,” *Proceedings of the Asia Pacific Microwave Conference*, Singapore, pp. 1894-1897, 2009.
- [16] X. H. Jin, X. D. Huang, C. H. Cheng, and L. Zhu, “Super-wideband printed asymmetrical dipole antenna,” *Progress In Electromagnetics Research Letters*, vol. 27, pp. 117-123, 2011.
- [17] M. S. Mahmud and S. Dey, “Design and performance analysis of a compact and conformal super wide band textile antenna for wearable body area applications,” *Proceedings of the 6<sup>th</sup> European Conference on Antennas and Propagation*, Czech Republic, pp. 1-5, 2012.
- [18] J. K. Liu, P. Esselle, S. G. Hay, and S. S. Zhong, “Study of an extremely wideband monopole antenna with triple band-notched characteristics,” *Progress In Electromagnetics Research*, vol. 123, pp. 143-158, 2012.
- [19] K. L. Lau, K. C. Kong, and K. M. Luk, “Super-wideband monopolar patch antenna,” *Electronics Letters*, vol. 44, no. 12, pp. 716-718, 2008.
- [20] K.-R. Chen, C.-Y.-D. Sim, and J.-S. Row, “A compact monopole antenna for super wideband applications,” *IEEE Antennas and Wireless Propagation Letters*, vol. 10, pp. 488-491, 2011.
- [21] M. Manohar, R. S. Kshetrimayum, and A. K. Gogoi, “Printed monopole antenna with tapered feed line, feed region and patch for super wideband applications,” *IET Microwaves, Antennas and Propagation*, vol. 8, pp. 39-45, 2014.
- [22] Y. Dong, W. Hong, L. Liu, Y. Zhang, and Z. Kuai, “Performance analysis of a printed super-wideband antenna,” *Microwave and Optical Technology Letters*, vol. 51, pp. 949-956, 2009.
- [23] J. Liu, K. P. Eselle, and S. S. Zhong, “A printed extremely wideband antenna for multi-band wireless systems,” *Antennas Propagation Society Symposium*, Toronto, Canada, July 2010.
- [25] M. N. Srifi, S. K. Podilchak, M. Essaïdi, and Y. M. M. Antar, “Compact disc monopole antennas for current and future ultra-wideband (UWB) applications” *IEEE Transactions on Antennas and Propagation*, vol. 59, no. 12, pp. 4470-4480, 2011.
- [25] C. C. Lin, P. Jin, and R. W. Ziolkowski, “Single, dual and tri-band-notched ultra-wideband (UWB) antennas using capacitively loaded loop (CLL) resonators,” *IEEE Transactions on Antennas and Propagation*, vol. 60, no. 1, pp. 102-109, 2012.
- [26] C. Yoon, W.-J. Lee, W.-S. Kim, H.-C. Lee, and H.-D. Park, “Compact band-notched ultra-wide band printed antenna using inverted L-slit,” *Microwave and Optical Technology Letters*, vol. 54, no. 1, pp. 143-144, 2012.
- [27] C. A. Balanis, *Antenna Theory: Analysis and Design*. 3<sup>rd</sup> ed., Wiley-Interscience: New York, NY, USA, 2012.



**Md. Moinul Islam** was born in Jhenidah, Bangladesh in 1983. He received B.Sc. and M. Sc. degrees in Information and Communication Engineering from Islamic University, Kushtia, Bangladesh in 2005 and 2006, respectively and a Ph.D. degree in Space Science from the

Universiti Kebangsaan Malaysia (UKM), Malaysia in 2016. He has authored or co-authored over 35 referred journals and conference papers. He is currently a Senior Lecturer at the Department of Software Engineering, Daffodil International University, Dhaka, Bangladesh. His research interests include antenna and wireless communications, metamaterials, medical imaging and sensing, satellite communications and radio frequency (RF).



**Mohammad Rashed Iqbal Faruque** was born in Chittagong, Bangladesh in 1974. He received the B.Sc. and M.Sc. degree in Physics from University of Chittagong, Chittagong, Bangladesh in 1998 and 1999, respectively, and a Ph.D. degree in Telecommunication Engineering

from the Universiti Kebangsaan Malaysia (UKM) in 2012. From July 2000 to until 2007, he worked as a Lecturer at Chittagong University of Engineering and Technology (CUET), Chittagong. From June 2007 to November 2008, he was an Assistant Professor at University of Information Technology and Sciences (UITS), Chittagong. He has authored or co-authored approximately 60 referred journals and conference

papers. He is currently a Senior Lecturer at the Institute of Space Science (ANGKASA), UKM, Malaysia. His research interests include the RF, electromagnetic field and propagation, FDTD analysis, electromagnetic radiation, metamaterials applications and electromagnetic compatibility.



**Mohammad Tariqul Islam** is a Professor at the Institute of Space Science of the Universiti Kebangsaan Malaysia (UKM). He is also the Group Leader of Radio Astronomy Informatics Group at UKM. Prior to joining UKM, he was a Lecturer in Multimedia University, Malaysia.

He is a Senior Member of the IEEE. He is serving as the Editor-in-Chief of the International Journal of Electronics & Informatics (*IJEI*). He has been very promising as a researcher, with the achievement of

several International Gold Medal awards, a Best Invention in Telecommunication Award and a Special Award from Vietnam for his research and innovation. He has been awarded “Best Researcher Award” in 2010 and 2011 at UKM. His professorial interests include the areas of communication antenna design, radio astronomy antennas, satellite antennas, and electromagnetic radiation analysis. He has published over 150 journal papers and few book chapters on various topics related to antennas, microwaves and electromagnetic radiation analysis. He also has filled 6 patent applications on communication antennas. Thus far, his publications have been cited 810 times, and the H-index is 18 (Source: Scopus). He is now handling many research projects from the Ministry of Science, Technology and Innovation (MOSTI), Ministry of Higher Education Malaysia (MOHE) and some International research grants from Japan.